

The Polar Sea Ice Cover from Aqua/AMSR-E

Fumihiko Nishio

Chiba University

Center for Environmental Remote Sensing

1-33, Yayoi-cho, Inage-ku, Chiba, 263-8522, Japan

fnishio@cr.chiba-u.ac.jp

Josefino C. Comiso

NASA Goddard Space Flight Center

Greenbelt, MD 20771, USA

fnishio@cr.chiba-u.ac.jp

josefino.c.comiso@nasa.gov

Abstract— Historical satellite data reveal that among the most remarkable manifestations of changes in the polar regions are the relatively rapid decline of 9 %/decade in the Arctic perennial ice cover and the 7%/decade retreat in the Bellingshaussen/Amundsen Seas ice cover in the Antarctic. The launch of the Advanced Multichannel Scanning Radiometer (AMSR-E) on board the EOS-Aqua satellite in 2002 has enabled the study the polar ice cover in greater detail and the evaluation of the accuracy and consistency of historical satellite data. The AMSR-E system has higher resolution and larger spectral range thereby providing ability to better assess the spatial distribution of different ice types in the marginal ice zones, the sizes and characteristics of sensible and latent heat polynyas, and the extent of ridging and divergence within the ice pack. Comparative analysis reveals that the sea ice data derived from AMSR-E are coherent and consistent with Moderate Resolution Imaging Spectroradiometer (MODIS) data on board the same satellite, especially when the 5-km resolution 89 GHz data are used. During the periods of overlapping coverage, the AMSR-E data are also shown to provide basically the same spatial and temporal variability as those from the Special Scanning Microwave Imager (SSM/I) which has been the key source of sea ice data since 1987. Quantitative comparative studies using AMSR-E and SSM/I data also reveal a clear indication of the advantage of the former in consistently identifying the 10-15% ice edge and in quantifying the regional and global sea ice extents. This is reflected in the calculation for the trend in ice extent when AMSR-E data is used instead of SSM/I data. However, the difference is within error and the estimate for the trend in ice area is in good agreement.

Keywords-AMSR-E,SSM/I, MODSI, sea ice extent ,ice edge

I. INTRODUCTION

Much of what we currently know about the large scale variability of the global sea ice cover has been derived from satellite passive microwave data (Parkinson et al., 1999; Bjorgo et al., 1999; Zwally, 2002; Comiso, 2002). This capability for studying sea ice has recently been enhanced considerably with the launched of the Advanced Microwave Scanning Radiometer in May 2002 on board the EOS-Aqua satellite (referred to as "AMSR-E") and in January 2003 on

board ADEOS-2 (called "AMSR"). The improvements over the Special Scanning Microwave Imager (SSM/I), which has been the primary source of data since July, 1987, include higher resolutions at all frequencies and a wider spectral range. In particular, AMSR-E and AMSR have resolutions of about 5 km at the 89 GHz channel and 12 km at the 36 GHz channel, while the corresponding values for SSM/I are 12 km and 25 km. Also, SSM/I has only 7 channels from 19 GHz to 89 GHz while AMSR-E has twelve channels from 6 GHz to 89 GHz, and AMSR has all the AMSR-E channels plus 50.3 and 52.8 GHz channels, primarily meant for atmospheric sounding. The lower frequency channels (6.9 and 10.65 GHz) provide the ability to retrieve Sea Surface Temperature (SST) and Surface Ice Temperature (SIT) that are useful not only as climate data sets but also in removing ambiguities in the retrievals due to atmospheric and surface temperature effects. Furthermore, the higher resolution minimizes the uncertainties associated with the use of mixing algorithms to retrieve geophysical parameters. Sea ice products derived from AMSR provided have been shown to be consistent with those from AMSR-E. For the purpose of this paper, we will use results primarily from AMSR-E which is the only sensor of the two that is currently providing data because of an unexpected demise of Midori-2 after 9 months of operation.

The study of sea ice also benefits from the availability of the Moderate Resolution Imaging Spectroradiometer (MODIS) on board the Aqua satellite which provides concurrent observation of the same surface as AMSR-E. With 36 channels in the visible and infrared frequencies, MODIS provides needed ancillary data to ensure that the interpretation of AMSR-E over sea ice is as accurate as possible. Some of the visible channels from MODIS have resolutions of 250 m, which is good enough to detect leads, polynyas and other small surface features that are inferred only indirectly from AMSR-E data. Validation of the latter is important since it is the AMSR-E that provides the spatial and temporal coverage needed for process studies. MODIS data cannot be used for the same purpose because of the persistence of cloud cover in the polar regions.

II. HEMISPHERIC RETRIEVALS OF SEA ICE PARAMETERS

The distributions of sea ice in both hemispheres are quite different in that sea ice is surrounded by land in the Arctic while sea ice surrounds the Antarctic continent. In the winter, the Arctic is basically covered by consolidated ice that are

| Report Documentation Page | | | | Form Approved OMB No. 0704-0188 | |
|--|------------------------------------|-------------------------------------|--|---|------------------------------------|
| Public reporting burden for the collection of information is estimated to average 1 hour per response, including the time for reviewing instructions, searching existing data sources, gathering and maintaining the data needed, and completing and reviewing the collection of information. Send comments regarding this burden estimate or any other aspect of this collection of information, including suggestions for reducing this burden, to Washington Headquarters Services, Directorate for Information Operations and Reports, 1215 Jefferson Davis Highway, Suite 1204, Arlington VA 22202-4302. Respondents should be aware that notwithstanding any other provision of law, no person shall be subject to a penalty for failing to comply with a collection of information if it does not display a currently valid OMB control number. | | | | | |
| 1. REPORT DATE 25 JUL 2005 | | 2. REPORT TYPE N/A | | 3. DATES COVERED - | |
| 4. TITLE AND SUBTITLE The Polar Sea Ice Cover from Aqua/AMSR-E | | | | 5a. CONTRACT NUMBER | |
| | | | | 5b. GRANT NUMBER | |
| | | | | 5c. PROGRAM ELEMENT NUMBER | |
| 6. AUTHOR(S) | | | | 5d. PROJECT NUMBER | |
| | | | | 5e. TASK NUMBER | |
| | | | | 5f. WORK UNIT NUMBER | |
| 7. PERFORMING ORGANIZATION NAME(S) AND ADDRESS(ES) Chiba University Center for Environmental Remote Sensing 1-33, Yayoi-cho, Inage-ku, Chiba, 263-8522, Japan | | | | 8. PERFORMING ORGANIZATION REPORT NUMBER | |
| 9. SPONSORING/MONITORING AGENCY NAME(S) AND ADDRESS(ES) | | | | 10. SPONSOR/MONITOR'S ACRONYM(S) | |
| | | | | 11. SPONSOR/MONITOR'S REPORT NUMBER(S) | |
| 12. DISTRIBUTION/AVAILABILITY STATEMENT Approved for public release, distribution unlimited | | | | | |
| 13. SUPPLEMENTARY NOTES See also ADM001850, 2005 IEEE International Geoscience and Remote Sensing Symposium Proceedings (25th) (IGARSS 2005) Held in Seoul, Korea on 25-29 July 2005. , The original document contains color images. | | | | | |
| 14. ABSTRACT | | | | | |
| 15. SUBJECT TERMS | | | | | |
| 16. SECURITY CLASSIFICATION OF: | | | 17. LIMITATION OF ABSTRACT UU | 18. NUMBER OF PAGES 5 | 19a. NAME OF RESPONSIBLE PERSON |
| a. REPORT unclassified | b. ABSTRACT unclassified | c. THIS PAGE unclassified | | | |

more confined, thicker and colder than those in the Antarctic. In the Arctic, a large fraction of the ice floes survives the summer melt and can be survived as old as 7 years, while in the Antarctic, it is rarely the case that an ice floe is older than 2 years, the reason being that the remnants of summer ice gets flushed out of the original location by strong ocean currents (e.g., Weddell gyre) during autumn and winter. Also, the impact of divergence in the Antarctic is stronger than in the Arctic because of the lack of an outer boundary in the former.

Sea ice is an inhomogeneous material consisting of ice, brine, air pockets, and other impurities, the relative percentages of which are different depending on formation conditions and history of the ice. Hemispherical differences in environmental conditions makes the

inhomogeneity of ice in the Arctic generally different from that in the Antarctic leading to differences in the dielectric properties and emissivity of sea ice in the two regions. This leads to differences in the brightness temperatures, especially for consolidated ice, making it necessary to have different input parameters for the algorithm used to retrieve sea ice products from the two hemispheres (Comiso et al., 2003).

Among the most basic geophysical cryospheric parameter that is derived from passive microwave data is sea ice concentration. Sea ice concentration, C_p , has been defined as the percentage fraction of sea ice within the field of view of the sensor. Such percentage is calculated using the mixing equation given by

$$T_b = T_i C_i + T_o (1 - C_i) \quad (1)$$

where T_b is the observed brightness temperature while T_i and T_o are the brightness temperature of sea ice and open water, respectively, in the region of observation. The sea ice algorithms are designed to obtain T_i and T_o as accurately as possible. The equation suggests that data from only one channel is required but variations in emissivity and temperature make it necessary to use a combination of two or more channels to obtain accurate retrievals (Svendsen et al, 1987; Gloersen et al, 1992; Comiso et al., 2003). Different techniques, however, can produce inconsistent results (Comiso and Steffen, 2001)

The first question to ask is how the AMSR ice data compares with those of historical data. To answer this question, ice concentration maps for both hemispheres and for the same mid-winter day were derived for AMSR-E and SSM/I data and are shown in Figure 1. The ice concentration values for the two are shown to be generally consistent both at the ice edge and within the pack. This is encouraging since it means that the AMSR-E data will provide a consistent continuation of historical sea ice data that already span at least 25 years. In these retrievals, the same set of channels, gridded in the same way was used. The difference between AMSR-E and SSM/I data is not so obvious. To illustrate the advantage of a higher resolution, Figure 2 shows a Landsat image over the Sea of Okhotsk which is compared with AMSR-E data at resolutions of 6.25 km, 12.5 km, and 25 km. It is apparent that much of the small scale details apparent in the Landsat image are also represented in the 6.25 GHz image. Some of the details are still there with the 12.5 km grid but much is

lost in the 25 km grid. Overall, however, the three ice images from AMSR-E provide consistent ice distributions in that the total extent and area of the ice cover are in good agreement. The additional details provided by the higher resolution data available with AMSR-E, however, provide the means to do process studies more accurately.

The higher resolution of AMSR also provide for a better definition of the marginal ice zone and a more precise location of the ice edge. To illustrate this, plots of brightness temperatures at different frequencies along a 35° W longitude transect over a marginal ice zone in the Antarctic for both AMSR and SSM/I are shown in Figure 3a and 3b, respectively. The plots show that the brightness temperatures are relatively low and uniform in the open water and gradually increase over the marginal ice zone and at their highest values over the ice pack. Over the ice edge, the AMSR brightness temperatures shows much more consistency for the different frequencies than the SSM/I brightness temperatures. The corresponding plots for ice concentration as shown in Figure 3c indicates that AMSR provides a more defined ice edge than SSM/I with the latter showing the effect of sidelobes and a bigger footprint.

III. SEA ICE EXTENT AND AREA IN THE TWO HEMISPHERE

For climate change studies, long historical records are always desired and this is possible for satellite measurements only by combining data from different satellites. It is thus important to find out how the new AMSR-E data compare with SSM/I data which have been the source of continuous sea ice data since July 1987. An example of such comparison has been shown in Figure 4 and it appears that there is generally a good consistency between AMSR-E and SSM/I ice concentration data. For more quantitative comparison, the sea ice extent and area of the global sea ice cover in both hemispheres are calculated using both AMSR-E and SSM/I ice concentration data. Ice extent is defined here as the sum of the areas of the data elements (pixels) with at least 15% ice concentration while ice area is the sum of the products of the area of each pixel and the corresponding ice concentration. The results from estimates of monthly ice extents are presented in Figure 4 for the period in which AMSR-E data have been available. It is apparent that the data points for each month from both sensors are in good agreement with the SSM/I data generally higher in values than the AMSR-E data. The deviations are likely in part due to the coarser resolution of the SSM/I compared with the AMSR-E sensor as illustrated in Figure 2. This in itself could also explain the higher deviation in the Arctic region, where the ice edges are longer, than in the Antarctic region. It is, however, encouraging that the seasonalities of the ice extents in both hemispheres as observed by both sensors are basically identical.

To assess how AMSR-E data can be used for studies in the interannual variability and trends in the ice cover, AMSR-E data are used in conjunction with SSM/I and SMMR data. To do this, the monthly ice extents and ice data from SMMR

and SSM/I are combined with those from AMSR-E data to produce a time series from October 1978 to the present. Averages of all data for each month was also generated to create monthly climatologies. These monthly climatologies were used to generate monthly anomalies which are differences between data for each month and the monthly climatology for the same month. The monthly anomalies for the ice extent, ice area and ice concentrations in the Northern Hemisphere are presented in Figure 5. Interannual fluctuation as high as $1 \times 10^6 \text{ km}^2$ is observed but a negative trend is apparent. For ice extent, the trend is shown to be $-3.24 \pm 0.20\%$ per decade while for ice area, it is $-3.45 \pm 0.20\%$ per decade. The ice concentration appears to be relatively uniform with the trend being only 0.03% per decade. For comparison, when the AMSR-E data is replaced by SSM/I data, the ice extent trend is $-2.87 \pm 0.19\%$ per decade while that for the ice area is $-3.47 \pm 0.20\%$ per decade. With SSM/I data the trend in ice concentration is $-0.08 \pm 0.01\%$ per decade. It is good to know that the trends in ice area are in very good agreement. There is a slight difference in the trend for the extent but they are basically associated with the aforementioned bias due to the lower resolution of the SSM/I data.

The corresponding anomaly plots for the Southern Hemisphere are shown in Figure 6. When the AMSR-E data is used, the trends in ice extent, ice area and ice concentrations are $0.57 \pm 0.24\%$ per decade, $1.35 \pm 0.28\%$ /decade and $0.08 \pm 0.01\%$ /decade, respectively. When only SMMR and SSM/I data are used only, the corresponding trends for the same time period are 0.74 ± 0.24 , 1.38 ± 0.27 and $0.07 \pm 0.01\%$ per decade. Again, the trends in ice area using either AMSR-E or SSM/I data are in very good agreement. The trend in ice extent is again slightly more positive when SSM/I other than AMSR-E data are used. Since this is consistent in both polar regions, the bias associated with the ice edge is likely a credible explanation.

IV. DISCUSSION AND CONCLUSIONS

The AMSR-E data provides data that are generally in good agreement with SSM/I data. The former, however, allows for opportunities to study the sea ice cover at higher accuracy and in greater spatial detail than ever before. The greater spectral range and higher resolution data set will enable more in depth studies of many mesoscale processes that occurs in polynyas, divergence areas and the marginal ice zones. Comparative studies shows a good match of high resolution AMSR-E data with those of other satellite data providing confidence that the interpretation of mesoscale features in the former are indeed accurate. The good matching for microwave data from different resolutions also suggests that results from analysis of AMSR-E data can be extrapolated to other years using historical data (e.g., SSM/I data). Having coincident measurements, like those of MODIS on board the same satellite also provide unlimited possibilities for the study of other processes within the ice pack and interactions between the ocean, ice and the atmosphere.

It is also good to know that the ice extents and ice areas calculated from AMSR-E and SSM/I are generally consistent.

The actual ice areas have better consistencies reflecting the agreement in ice concentration values that are calculated from the two sensors. A small bias is observed in the calculation of ice extent, likely caused by the coarser resolution of the SSM/I data. These results become more apparent when trends in the ice cover are calculated using historical data. It is good to find out that the ice cover is good consistency in the trends using either SSM/I or AMSR-E data. There is a slight bias when trends in ice extent is estimated but we know that this is because of the higher resolution of the AMSR-E data. This bias could probably be minimized by making slight adjustments in the algorithm for estimating ice concentrations from the SSM/I data.

Needless to say, it is always prudent to do extensive validations for derived data from new sensors to establish absolute accuracy and precision. Validation studies are ongoing in both hemispheres, but we are confident that AMSR-E is a big improvement over previous passive microwave sensors.

REFERENCES

- Bjorgo, E., O.M. Johannessen and M.W. Miles, "Analysis of merged SSMR-SSM/I time series of Arctic and Antarctic sea ice parameters 1978-1995", *Geophys. Res. Lett.*, Vol. 24, pp. 413-416, 1997.
- Comiso, J. C., A rapidly declining Arctic perennial ice cover, *Geophys. Res. Letts.*, 29(20), 1956, doi:10.1029/2002GL015650, 2002.
- Comiso, J. C., D. J. Cavalieri and T. Markus, Sea ice concentration, ice temperature, and snow depth, using AMSR-E data, *IEEE TGRS*, 41(2), 243-252, 2003.
- Comiso, J.C., and K. Steffen, Studies of Antarctic sea ice concentrations from satellite data and their applications, *J. Geophys. Res.*, 106(C12), 31361-31385, 2001.
- Gloersen P., W. Campbell, D. Cavalieri, J. Comiso, C. Parkinson and H.J. Zwally, Arctic and Antarctic Sea Ice, 1978-1987: Satellite Passive Microwave Observations and Analysis, *NASA Spec. Publ. 511*, 1992.
- Kumerow, C., On the accuracy of the Eddington approximation for radiative transfer in the microwave frequencies", *J. Geophys. Res.*, Vol. 98, pp. 2757- 2765, 1993.
- C. Matzler, C., R. O. Ramseier and E. Svendsen, "Polarization effects in sea ice signatures", *IEEE J. Oceanic Engineering*, Vol. OE-9, pp. 333-338, 1984.
- Parkinson, C.L., D.J Cavalieri, P. Gloersen, H.J. Zwally and J.C. Comiso, Arctic sea ice extents, areas, and trends, 1978-1996, *J. Geophys. Res.*, 104(C9), 20837-20856, 1999.
- Svendsen, E., C. Matzler and T.C. Grenfell, "A model for retrieving total sea ice concentration from a spaceborne dual-polarized passive microwave instrument operating near 90 GHz", *Int. J. Rem. Sens.*, Vol. 8, pp. 1479-1487, 1987.
- Zwally, H.J., J.C. Comiso, C. Parkinson, D. Cavalieri and P. Gloersen, Variability of the Antarctic sea ice cover, *J. Geophys. Res.* 107(C5), 1029-1047, 2002.

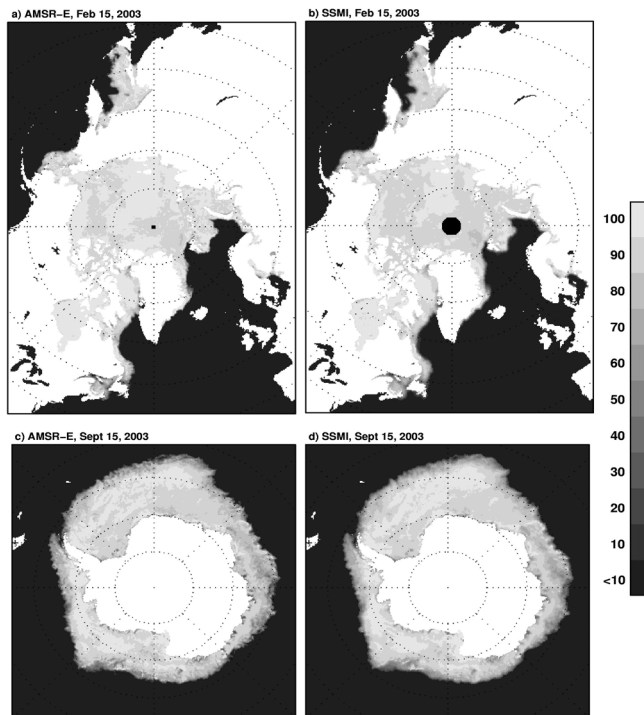


Figure 1. Daily ice concentration maps during winter in the (a) Northern Hemisphere using AMSR-E data; (b) Northern Hemisphere using SSM/I data; (c) Southern Hemisphere using AMSR-E data; and (d) Southern Hemisphere using SSM/I data.

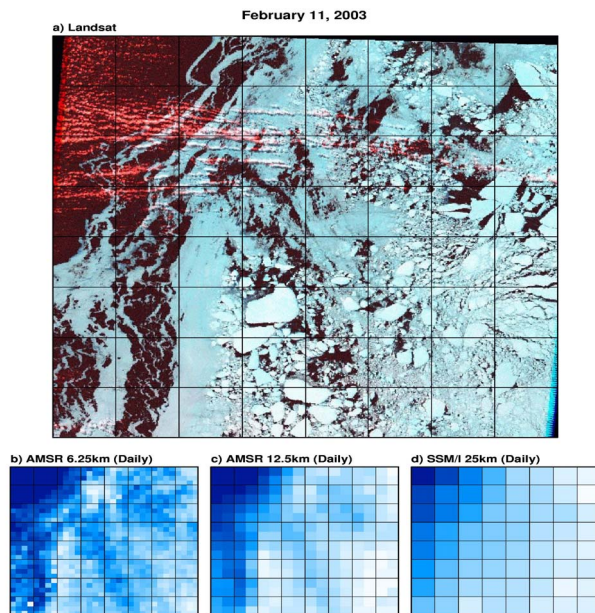


Figure 2. (a) Landsat-7 image of the ice cover in the Okhotsk sea and corresponding AMSR ice concentration maps at (b) 6.25 km grid as derived from the 89 GHz channels; (c) 12.5 km grid as derived using the AMSR bootstrap algorithm and (d) 25 km grid as derived using the AMSR bootstrap algorithm.

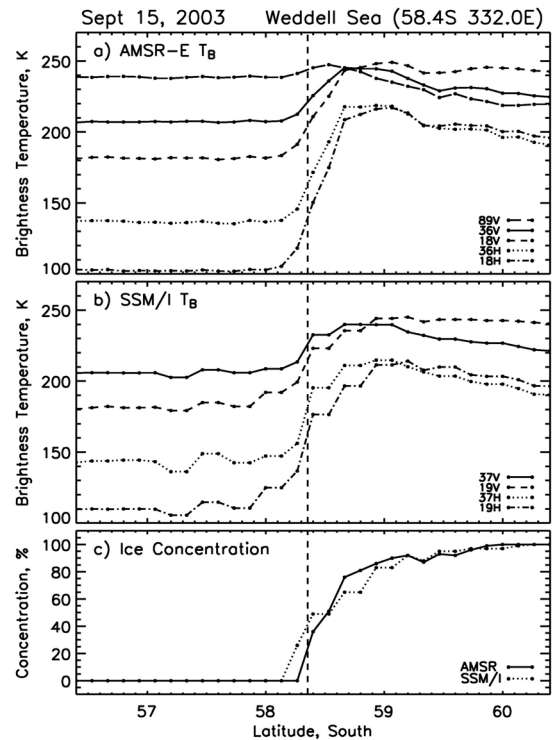


Figure 3. Brightness temperatures using (a) AMSR-E and (b) SSM/I data and (c) ice concentrations from AMSR-E and SSM/I data along a transect through the ice edge.

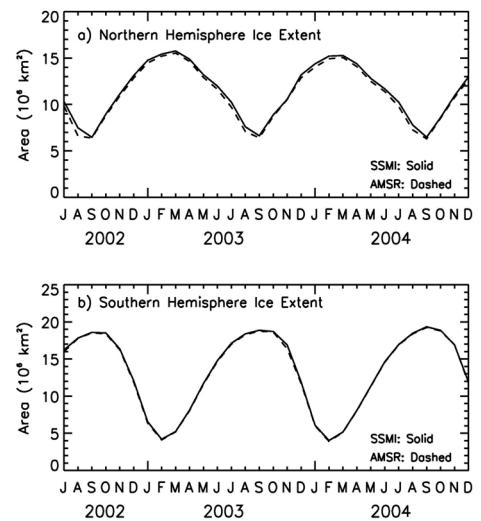


Figure 4. Comparison of total ice extents inferred from AMSR-E and SSM/I in (a) northern hemisphere and (b) southern hemisphere.

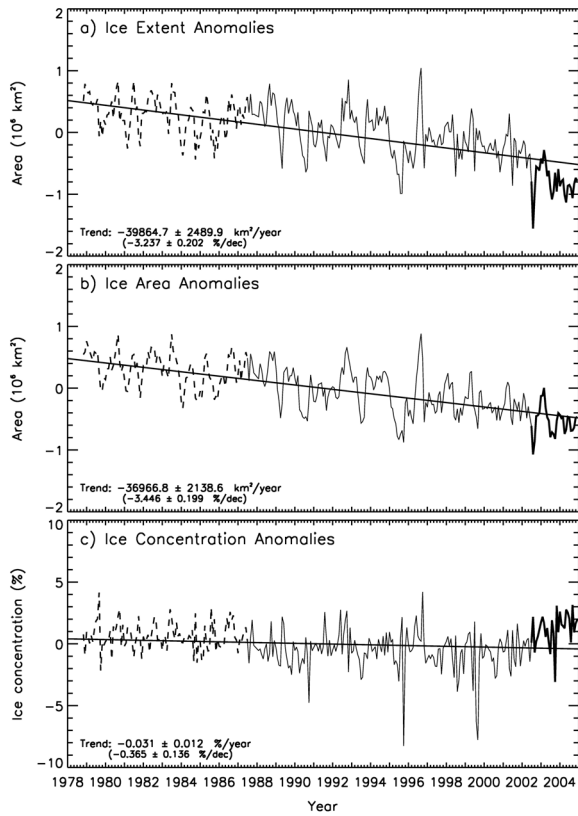


Figure 5. Anomalies and trends using AMSR-E and SSM/I monthly data on (a) ice extent; (b) ice area; and (c) ice concentration in the Northern Hemisphere.

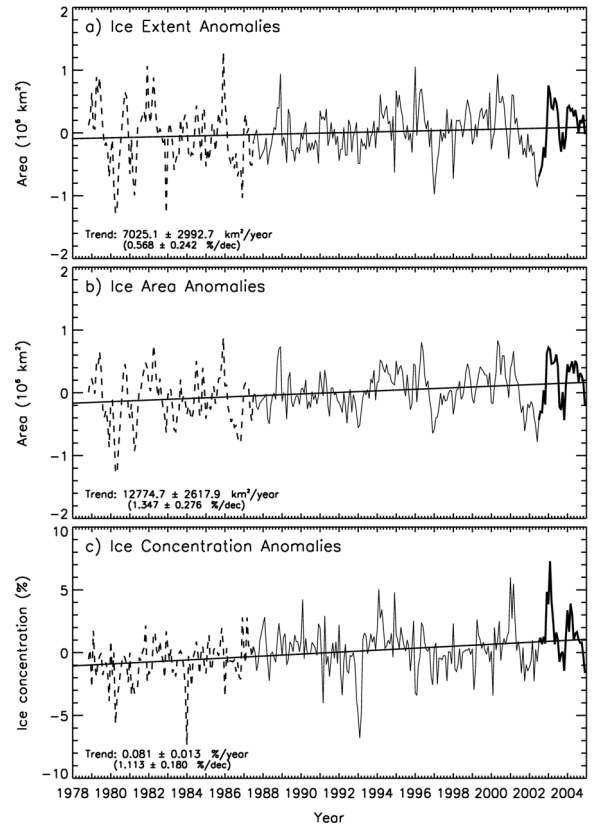


Figure 6. Anomalies and trends using AMSR-E and SSM/I monthly data on (a) ice extent; (b) ice area; and (c) ice concentration in the Southern Hemisphere.